JOURNAL OF GEOPHYSICAL RESEARCH, VOL. 106, NO. D11, PAGES 12,183–12,191, JUNE 16, 2001

Deuterium in water vapor evaporated from a coastal salt marsh

Hui He[1]
Department of Geology and Geophysics, Yale University, New Haven, Connecticut

Xuhui Lee
School of Forestry and Environmental Studies, Yale University, New Haven, Connecticut

Ronald B. Smith
Department of Geology and Geophysics, Yale University, New Haven, Connecticut

Abstract. Atmospheric water vapor was sampled simultaneously at two heights in the atmospheric surface layer above a coastal salt marsh near New Haven, Connecticut, during June 11–27, 1997. The water vapor samples were analyzed for their mixing ratio, Q, and deuterium isotope ratio, δD. The observed δD varied in the range of -145 to -89 per mil and was positively correlated with Q, reflecting the influence of in-cloud condensation and surface evapotranspiration processes at a regional scale. Both Q and δD were, in general, lower at the upper level, indicating an upward transport of $H_2{}^{16}O$ and $HD^{16}O$. The Craig-Gordon model reproduced reasonably well the combined effects of equilibrium and kinetic fractionations and atmospheric demand on the evaporation process. Transpiration of the marsh plants, *Spartina patens* (Ait.), was a minor component (11%) of the total evapotranspiration during the experimental period. We also suggest that the relationship between δD and salinity, S, of the marsh surface water can be used to infer the isotope flux ratio. More data, however, are needed to verify this mass balance approach.

1. Introduction

The stable water isotopes, deuterium (D) and oxygen 18 (^{18}O), are important tracers of the natural hydrological processes [*Friedman et al.,* 1964; *Craig and Gordon,* 1965; *Clark and Fritz,* 1997]. These environmental isotopes have been used widely in studies of paleoclimatology [*Merlivat and Jouzel,* 1979; *Jouzel et al.,* 1982, 1987], cloud physics [*Jouzel and Merlivat,* 1984; *Jouzel,* 1986], atmospheric water vapor transport [*Smith,* 1992], and ecosystem processes [*Yakir and Sternberg,* 2000].

The abundance of D or ^{18}O is commonly represented by its relative deviation from a known standard, standard mean ocean water (SMOW), as

$$\delta = \left(\frac{R - R_{\mathrm{SMOW}}}{R_{\mathrm{SMOW}}}\right) 1000, \qquad (1)$$

where R is the isotope ratio by molar volume and R_{SMOW} is the isotope ratio of $HD^{16}O$ or $H_2{}^{18}O$ of SMOW. Water vapor evaporated from the surface carries isotopic signatures of the evaporating surface source [*He and Smith,* 1999b].

The scalar concentrations in the atmospheric boundary layer (ABL) show strong gradients in the inversion (entrainment) layer and in the surface layer, which are separated by the mixed layer where gradients are small because of vigorous turbulent mixing. In their study about water vapor transport through the ABL, *He and Smith* [1999a] measured deuterium and oxygen 18 isotope ratios in the ABL and developed a mixing line method to find the isotopic characteristics of the water vapor evaporated from the New England forests. Their mixing line method takes advantage of the vertical gradients at the top of ABL. Because the air mass far above the surface acquires the characteristics of the underlying surface over a broad source region, this so-called ABL top method is not suitable for characterizing localized surface sources.

In this companion study, we focus on the atmospheric surface layer over a coastal salt marsh. There are a number of reasons why the salt marsh was chosen as the study site. Experimental study of the $HD^{16}O$ flux

[1]Now at Raytheon Information Technology and Scientific Services, Lanham, Maryland.

Paper number 2001JD900080.
0148-0227/01/2001JD900080$09.00

is possible because sufficient gradient of $HD^{16}O$ exists in this layer owing to ample water supply for evaporation. The temporal evolution of δD and salinity S of the marsh surface water enables us to use S as a tracer to understand the fractionation during evaporation. Finally, comprehensive observation of micrometeorology was already in place as part of another project [*Lee et al.*, 2000].

The isotopic composition of the evapotranspiring water vapor, δD_F, can be expressed as

$$\delta D_F = F_T (\delta D_T - \delta D_E) + \delta D_E, \quad (2)$$

where F_T is the fraction of transpiration (water loss via plant stomata) and δD_T and δD_E are isotopic compositions of transpiring vapor and evaporating vapor (vapor from surface water and soil), respectively. It is a well-established fact that water uptake by roots and subsequent transpiration are not discriminative [*Ehleringer and Dawson,* 1992]. Evaporation, in contrast, favors a faster loss of the lighter isotope $H_2{}^{16}O$ because of the equilibrium and kinetic fractionation effects. Atmospheric variables such as humidity and isotopic composition of the ambient moisture exert some influence on the evaporation and fractionation processes. In the simple case of isolated water bodies at steady state with the atmosphere, *Craig and Gordon* [1965] proposed a resistance analogy for water movement across the water-air interface and derived the following model for the isotopic composition of the evaporating water, δD_E:

$$\delta D_E = \frac{\delta D_e - h\delta D - (1-h)(1-\alpha_k)}{(1-h) + (1-h)(1-\alpha_k)}, \quad (3)$$

where δD_e is an equilibrium isotope ratio to be defined in section 3.3, h is the relative humidity defined as the ratio of the actual water vapor pressure to the saturation vapor pressure at water temperature, δD is the isotope composition of the ambient water vapor, and α_k is a kinetic fractionation factor. Improvements to this model are given by *He and Smith* [1999b], *Flanagan and Ehleringer* [1991], *White* [1988], and others. Models of this type have been extensively tested in laboratory conditions [*Roden and Ehleringer,* 1999]. Our study appears to be the first attempt at evaluating (3) in field conditions.

The objectives in this paper are threefold: (1) to report the first results of the deuterium isotope ratios of atmospheric water vapor at a coastal salt marsh, (2) to characterize the deuterium isotope flux ratio using a mixing line method developed by *He and Smith* [1999a], and (3) to interpret the influence of environmental factors on the derived deuterium isotope flux ratios.

There are numerous studies on using water isotopes as tracers to understand water movement in the soil-plant-atmosphere continuum (see the recent review by *Yakir and Sternberg* [2000]). Most of these studies were conducted on individual leaves or plants in laboratory settings. Our research is among the few studies that investigate the fluxes of isotopes at an ecosystem scale [*Brunel et al.,* 1992; *Yakir and Wang,* 1996; *Bowling et al.,* 1999].

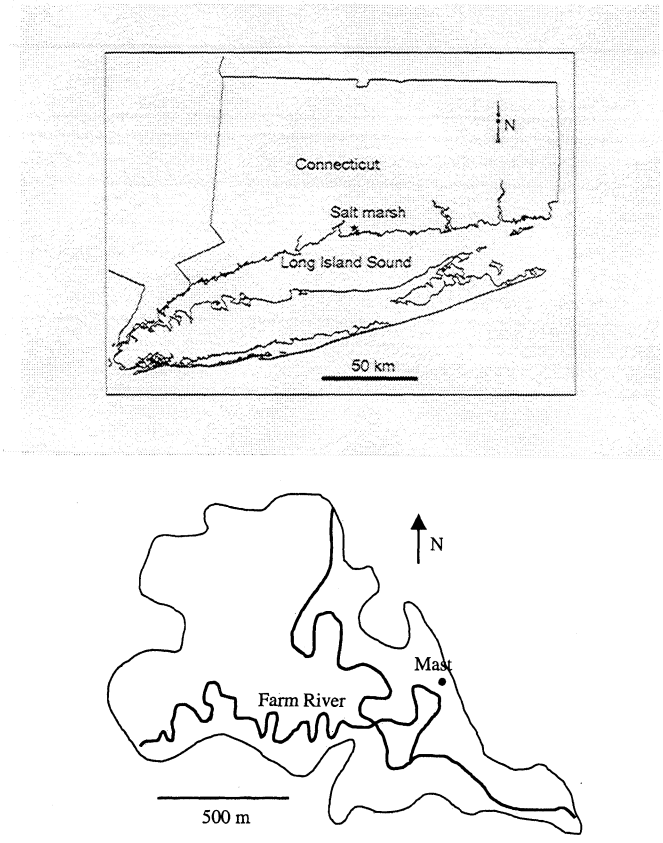

Figure 1. Maps of the Farm River salt marsh near New Haven, Connecticut. The boundary line in the lower map indicates the edge of the salt marsh. The mask sees mainly the land surface instead of the salt marsh when the wind comes from directions of north, northeast, and east. Good fetch corresponds to wind directions between 120° and 300°.

2. Methodology

2.1. Site

The site was the Farm River salt marsh (72°52′W, 41°16′N) 1.5 km away from Long Island Sound. Figure 1 sketches the location of the site. The marsh grass, *Spartina patens* (Ait.), was 30 – 40 cm tall at the time of the experiment. Fetch was good (150 – 400 m) when the surface wind was in the range of 120°–300°. The site was inundated twice a day by tidal water. One kilometer upstream of the salt marsh is a freshwater lake, Lake Saltonstall. A schematic diagram of the salt marsh site is shown in Figure 2. The isotope and salinity characteristics of the marsh water are controlled by the amount of mixing between ocean water and fresh on-land water. Dead plant residue was a prominent feature of the marsh surface. The plant area index, including the dead residue, was 2.4, with an average canopy height of 0.3 m. The aerodynamic surface roughness was ~2 cm. Features in Figure 2 are not drawn to scale. More information about the site is given by *Lee et al.* [2000].

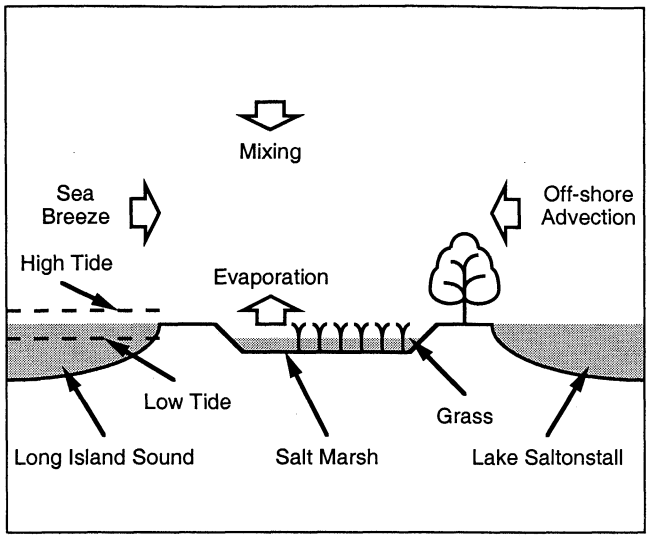

Figure 2. Schematic diagram of the salt marsh site. Features are not drawn to scale.

2.2. Water Vapor Collection

The configuration of the sampling system is shown in Figure 3. Two air inlets were located on a micrometeorological mast, which was 30 m away from the shore, at 88 cm and 276 cm above the sediment surface. Air was drawn from these two inlets by an air blower through two 40-m long polyvinyl chloride (PVC) pipes (inner diameter 2.54 cm) at a flow rate of 19.8 L s^{-1}. The travel time of air from the inlets to the dry-ice-cooled sampling canisters was ~2 s. Flow in the pipes was turbulent (Reynolds number = 3.36×10^4). A small fraction of the airstream was split to the sampling canister at a flow rate of 5.2 L min^{-1} maintained by two identical critical orifices. The collection efficiency of the canisters was close to 100% [*He and Smith,* 1999a].

Five sampling operations were performed on June 11, 15, 18, 21, and 27 (day of year 162, 166, 169, 172, and 178) and are denoted as SMEX–01, SMEX–02, SMEX–03, SMEX–04, and SMEX–05, respectively. During each operation a series of water vapor sample pairs were collected at 88-cm and 276-cm levels. For each sample pair, air was allowed to flow through two canisters (one for each inlet) simultaneously for 30 min. In the middle of the 30-min period a surface water sample was collected from the marsh for later analysis of its deuterium isotope ratio, δD, and salinity, S. Deuterium isotope ratios of atmospheric water vapor and marsh water samples were analyzed on a mass spectrometer at Yale University [*He and Smith,* 1999a]. The analytical precision is ±2.1 per mil (worst case).

2.3. Micrometeorological Measurements

We measured wind speed and direction, temperature, humidity, and global and net radiation on the mast (Figure 1). The three-dimensional wind was measured by a sonic anemometer/thermometer (Model 1012R2A, Gill Instruments). Temperature was measured at the two sampling levels using two fast-response thermocouple thermometers. The humidity measurement was carried out by measuring the dew point of the air sampled at the 88-cm level using a chilled mirror hygrometer (Model D2, General Eastern). A fast-response hygrometer (Model K20, Campbell Scientific) was mounted together with the sonic anemometer for water vapor flux measurement. The eddy correlation system (sonic anemometer/thermometer and fast-response hygrometer) was located at the 264-cm level above the sediment surface. The vertical fluxes of sensible heat, momentum, and moisture were obtained from the eddy correlation method.

Figure 4 is a plot of micrometeorological variables observed on June 11, 1997 (SMEX–01). The diurnal pattern shown here is also typical of other SMEX days. Shortly after sunrise, the surface layer above the salt marsh became convective, as indicated by positive sensible heat flux and higher temperature closer to the surface. The residue of dead plants of previous growth resulted in significant mulching effect as evidenced by the large sensible heat flux during the daytime. Latent heat flux was, in general, no greater than sensible heat flux despite ample water supply. On this particular date, the onset of sea breeze occurred at ~0800 LT, and the fetch for the remainder of SMEX–01 was favorable (>200 m). Typical friction velocity during the experiment was 0.3 m s^{-1}.

3. Results and Discussion

3.1. Mixing Ratio Correction

When using the actual sample size m_c, the water vapor mixing ratio can be calculated by

$$Q = \frac{m_c}{m_a}, \tag{4}$$

where m_a is the total mass of dry air flowing through the canister and can be calculated as [*Daneshyar,* 1976]

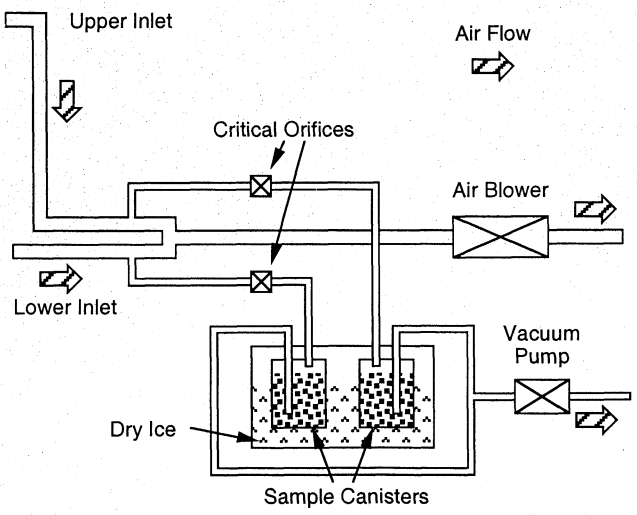

Figure 3. Schematic diagram of the water vapor sampling system. Sampling canisters are described by *He and Smith* [1999a].

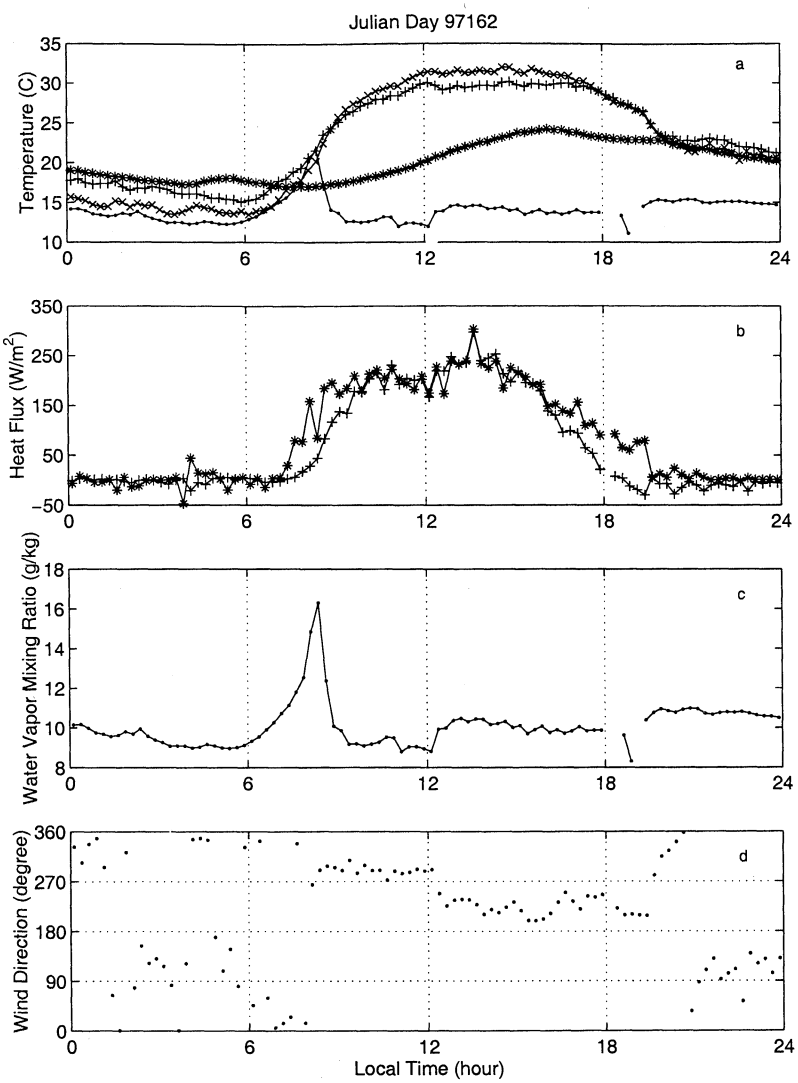

Figure 4. Micrometeorological data during SMEX–01 showing the diurnal variation of (a) air temperature at 276 cm (plus) and at 88 cm (cross), sediment temperature (asterisk), and dew point temperature at 88 cm (dot); (b) sensible heat flux (plus) and latent heat flux (asterisk) from the salt marsh; (c) water vapor mixing ratio at 88 cm; (d) wind direction at 264 cm. Each data point represents a 15-min average.

$$m_a = 1.28\frac{Apt}{\sqrt{c_p T}}, \tag{5}$$

in which $A = 4.32 \times 10^{-4}$ m^2 is the cross area of the critical orifice, $c_p = 1004$ J kg^{-1} K^{-1} is the specific heat of dry air at constant pressure, T is the air temperature, and $t = 30$ min is the length of sampling period for each sample [*He,* 1998]. It should be noted that p is not equal to the atmospheric pressure because the blower must exert a negative pressure with respect to ambient air (see Figure 3). The average pressure drop was 92.1 mbars.

Figure 5 is a plot of the mixing ratio calculated from the dew point temperature, $\tilde{Q}$, versus the mixing ratio calculated from (4). Of the 30 vapor samples taken at the 88-cm height, four were collected through a partially clogged critical orifice, as indicated by the squares to the left of the fitted line. Clogging of the critical orifice was visually identified in the field. Another outlier to the right of the fitted line, indicated by the triangle, was caused by malfunction of the dew point hygrometer. The remaining 25 samples give a linear fit of $\tilde{Q} = 1.007Q + 0.698$ with $R^2 = 0.99$. In Table 1 the mixing ratios at both the 88-cm and 276-cm levels are calculated from (4) followed by this regression equation.

3.2. Deuterium of Atmospheric Water Vapor

The observed δD varied in the range of -145 to -89 per mil (Table 1). This variation is highly correlated with Q, as shown in Figure 6. In Figure 6, we also plot data obtained over a grass canopy and a forest in Connecticut [*He,* 1998] to increase the range of data coverage. A least squares fit of the salt marsh data gives $\delta\mathrm{D} = -161.6 + 4.80\,Q$ with $R^2 = 0.66$. In general, drier air has had more vapor removed by in-cloud condensation and precipitation, a process that preferentially depletes the heavier isotope [*White and Gedzelman,* 1984]. Hence a positive correlation should exist

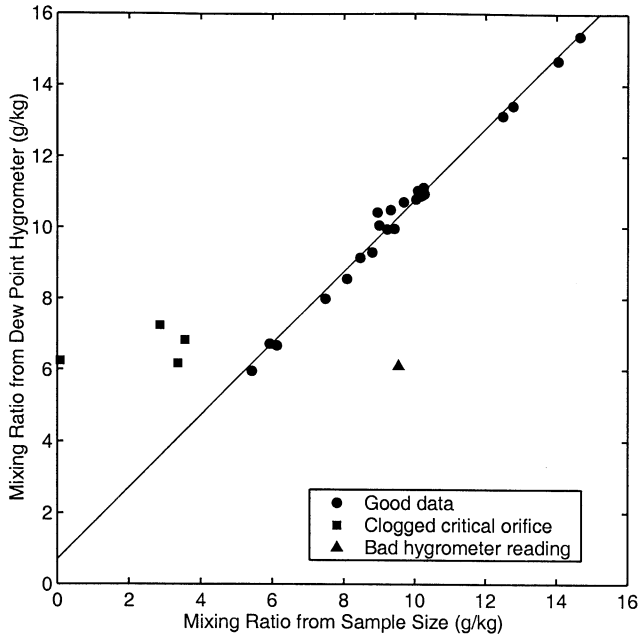

Figure 5. Plot of the mixing ratio derived by the dew point hygrometer versus the mixing ratio calculated from the sample size. The straight line represents a linear fit of $\tilde{Q} = 1.007Q + 0.698$ with $R^2 = 0.99$.

between δD and Q. The slope of regression of our data is much larger than that of *White and Gedzelman* [1984]. The reason for the difference is yet to be understood. It should be emphasized that variations in δD and Q reflect the influence of air mass at a regional scale, and hence the pattern shown in Figure 6 does not suggest the controls of evapotranspiration from the marsh surface.

3.3. Deuterium of Evapotranspiring Water Vapor

He and Smith [1999a] show that Q and δD at any two heights in a region dominated by turbulent mixing should form a unique mixing line in the δD – $1/Q$ domain. The intercept of this mixing line with the δD axis marks the isotope flux ratio or isotopic composition of the surface evapotranspiration, which is defined as [*He and Smith,* 1999b]

$$\delta \mathrm{D}_F = \left(\frac{1}{j R_{\mathrm{SMOW}}} \frac{F_D}{F} - 1 \right) 1000, \qquad (6)$$

where $j = 19/18$ is the ratio of molecular weights of $\mathrm{HD^{16}O/H_2{}^{16}O}$ and F and F_D are vertical mass fluxes of $\mathrm{H_2{}^{16}O}$ and $\mathrm{HD^{16}O}$, respectively. In this paper, the same mixing line approach is used to determine $\delta \mathrm{D}_F$ for the salt marsh. The assumption underlying the approach is that eddy diffusion is equally efficient in transporting both $\mathrm{H_2{}^{16}O}$ and $\mathrm{HD^{16}O}$ [*Yakir and Wang,* 1996]. This assumption should hold in the surface layer with adequate fetch.

The computed $\delta \mathrm{D}_F$ is given in Table 1. Also listed in Table 1 is the equilibrium isotope ratio, defined as the isotope ratio of water vapor in equilibrium with the condensed phase and computed as

$$\delta \mathrm{D}_e + 1000 = \frac{1}{\alpha_e} (\delta \mathrm{D}_s + 1000), \qquad (7)$$

where $\delta \mathrm{D}_s$ is the isotope ratio of the marsh surface water (Table 1) and the equilibrium fractionation factor α_e is a function of water temperature T_s (°C) [*Jouzel,* 1986]

$$\ln \alpha_e = \frac{24844}{(T_s + 273.15)^2} - \frac{76.248}{(T_s + 273.15)} + 0.052612.$$

As with other turbulent fluxes, $\delta \mathrm{D}_F$ has a footprint of several hectares. Two criteria should be used to judge the validity of the flux ratio. The first one is fetch requirement. The flux and gradient footprints will extend beyond the salt marsh at times when fetch is poor. For example, during SMEX–05, wind was blowing from the north, and consequently, the footprint lay over the land vegetation instead of the salt marsh (Figure 1). The averaged flux ratio for SMEX–05 is −48 per mil, which is much less negative than other periods and much less negative than the equilibrium ratio of the marsh water and may be indicative of the influence of transpiration of the upland vegetation. The impact of fetch is also obvious in the scatterplots shown in Figure 7.

To properly interpret the flux ratio data, the reader should also bear in mind the role of plant transpiration which does not discriminate against heavy isotopes and which should carry the isotopic signature of the source water [*Ehleringer and Dawson,* 1992]. Thus isotopic composition of the transpiring vapor, $\delta \mathrm{D}_T$, approximated by that of the marsh water, $\delta \mathrm{D}_s$, varied in

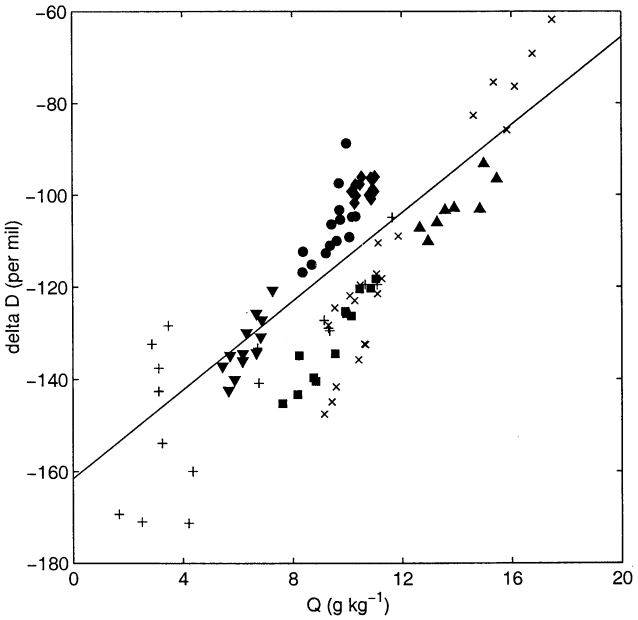

Figure 6. Scatterplot of deuterium isotope ratio of water vapor versus water vapor mixing ratio for SMEX–01 (circles), SMEX–02 (triangles down), SMEX–03 (diamonds), SMEX–04 (triangles up) and SMEX–05 (squares). Also shown are data obtained over a grass canopy (cross) and over a forest (plus) in Connecticut [*He,* 1998]. The straight line represents a linear fit of the salt marsh data of $\delta \mathrm{D} = -161.6 + 4.80\,Q$ with $R^2 = 0.66$.

Table 1. Summary of All SMEX Data

Time[a]	Q_t[b]	δD_t[c]	Q_b[d]	δD_b[e]	δD_F[f]	δD_s[g]	δD_e[h]	T_s[i]	Q_h[j]	S[k]	Fetch
					SMEX-01 (day of year 162)						
0700	9.62	−110.0	10.08	−109.2	−91.7	−22.6	−102.4	16.8	10.50	19.2	poor
0900	9.43	−106.4	10.19	−104.8	−84.8	−24.1	−96.6	24.2	9.97	19.6	good
1100	8.37	−116.8	9.22	−112.7	−72.1	−22.7	−92.5	27.2	9.15	20.6	good
1300	9.37	−111.0	9.70	−97.5	285.8	−16.1	−80.5	34.0	10.43	21.5	good
1500	8.38	−112.4	9.75	−105.4	−62.9	−9.1	−77.3	30.1	10.07	23.6	good
1700	8.70	−115.2	9.98	−88.8	91.0	−25.3	−96.0	26.0	9.96	19.3	good
1900	9.72	−103.3	10.31	−104.7	−127.2	−28.9	−101.0	24.2	6.11	18.5	good
					SMEX-02 (day of year 166)						
0700	5.44	−137.2	6.83	−130.8	−106.0	−23.5	−109.5	10.8	6.83	21.0	poor
0900	5.72	−134.9	6.25	—	—	—	—	18.4	6.25	—	poor
1100	5.67	−142.4	6.17	−136.0	−64.5	−26.1	−96.4	26.4	5.96	18.2	poor
1300	5.88	−140.1	6.18	−134.5	−22.9	—	—	29.6	6.18	—	good
1500	6.32	−129.9	6.88	−127.1	−95.6	−17.8	−88.6	26.6	6.68	21.3	good
1700	6.67	−134.3	6.67	−125.8	—	—	—	25.4	6.72	—	good
1900	7.27	−120.7	7.25	—	—	−30.2	−105.1	21.2	7.25	14.6	good
					SMEX-03 (day of year 169)						
1000	10.31	−97.8	10.89	−100.8	−153.9	−21.2	−98.6	19.3	11.00	19.1	good
1100	10.28	−101.7	10.95	−98.8	−53.4	—	—	19.6	10.89	—	good
1200	10.33	−100.2	10.88	−96.4	−24.0	−27.9	−104.1	20.0	10.95	16.6	good
1300	10.17	−99.3	10.80	−100.1	−112.6	−25.6	−102.3	19.7	10.80	17.6	good
1400	10.53	−96.2	11.02	−96.1	−94.1	—	—	19.9	11.13	—	good
1500	10.48	−97.7	11.00	−99.2	−131.2	−27.1	−104.0	19.3	10.92	18.6	good
					SMEX-04 (day of year 172)						
1000	12.65	−107.2	13.28	−106.0	−81.7	−20.1	−89.5	27.9	13.14	22.8	good
1200	12.96	−110.1	13.58	−103.4	37.9	−27.1	−99.5	24.1	13.43	19.9	good
1400	13.91	−102.9	14.85	−103.1	−106.5	−27.0	−97.0	26.7	14.69	18.6	good
1500	14.99	−93.2	15.47	−96.5	—	—	—	26.9	15.38	—	good
					SMEX-05 (day of year 178)						
0800	9.97	−125.9	10.46	−120.5	−10.8	−15.3	−91.8	20.7	10.72	22.5	poor
0900	9.93	−125.3	10.86	−120.3	−66.2	−16.6	−91.3	22.4	11.04	22.8	poor
1000	10.15	−126.3	11.04	−118.3	−26.4	−22.4	−93.6	25.8	10.95	23.2	poor
1100	8.77	−139.7	9.56	−134.5	−76.3	−20.2	−90.4	27.0	9.31	23.6	poor
1200	8.18	−143.3	8.85	−140.4	−105.1	−20.4	−88.3	29.6	8.56	23.9	poor
1300	7.64	−145.3	8.24	−134.9	−3.1	−24.6	−90.6	31.5	7.99	24.4	poor

[a]Centered time (LT) of 30-min sample collection.
[b]Water vapor mixing ratio estimated from the sample size at the upper level (276 cm) in g kg^{-1}.
[c]Water vapor deuterium isotope ratio at the upper level (276 cm) in per mil.
[d]Water vapor mixing ratio estimated from the sample size at the lower level (88 cm) in g kg^{-1}.
[e]Water vapor deuterium isotope ratio at the lower level (88 cm) in per mil.
[f]Deuterium isotope flux ratio calculated from the mixing line method in per mil.
[g]Deuterium isotope ratio of the surface marsh water in per mil.
[h]Equilibrium deuterium isotope ratio at marsh water temperature T_s in per mil.
[i]Marsh water temperature in °C.
[j]Water vapor mixing ratio at the lower level (88 cm) calculated from the dew point temperature in g kg^{-1}.
[k]Salinity of surface marsh water in per mil.

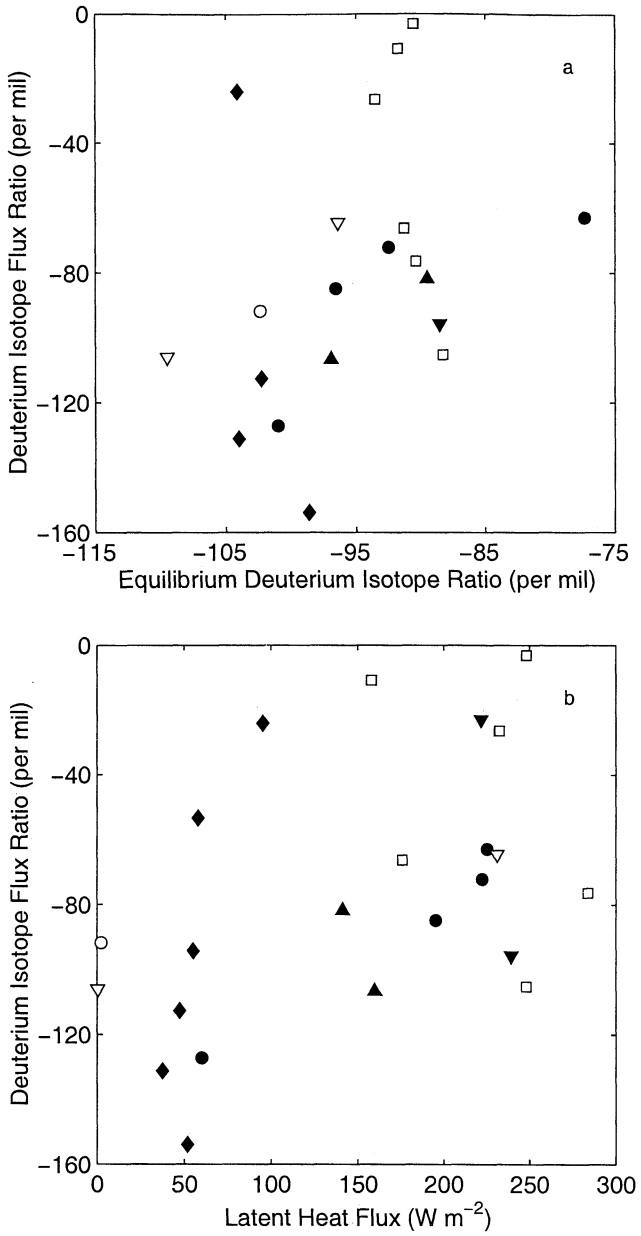

Figure 7. Plots of the derived deuterium isotope flux ratio versus (a) the deuterium isotope ratio of water vapor in equilibrium with surface water and (b) latent heat flux for SMEX–01 (circles), SMEX–02 (triangles down), SMEX–03 (diamonds), SMEX–04 (triangles up), and SMEX–05 (squares). Solid symbols indicate data with good fetch, and open symbols indicate data with poor fetch.

the range of −30 to −9 per mil during the experiment. Since δD_F cannot exceed δD_T according to (2), the positive flux ratio at 1300 and 1700 LT during SMEX–01 and at 1200 LT during SMEX–04 (Table 1) must have been caused by experimental errors.

Figure 7a plots the flux ratio versus the equilibrium isotope ratio of the marsh water for observations with negative δD_F. The outlier on the upper left corner (1200 LT, SMEX–03 in Table 1) has a flux ratio of −24 per mil, which is close to the isotopic ratio of the marsh water. This is possible only if evaporation was a negligible contributor to the total evapotranspiration according to (2) and contradicts the fact that environmental conditions favored fast evaporation. The observation was made during a tidal inundation (Table 2) at a net radiation flux of 300 W m^{-2}. For this reason we believe that the data point was biased by measurement error. The remaining data with good fetch give a linear correlation coefficient of 0.578 which is significant at a confidence level of 0.01. The statistically significant correlation confirms our expectation that equilibrium fractionation should play a large role in the evapotranspiration process of the marsh.

Figure 7b plots δD_F as a function of the total evapotranspiration rate measured with the eddy correlation. A less negative δD_F seemed to occur at times of high evaporation rate, suggesting either that at these times transpiration became more important or that evapotranspiration rate was correlated with other variables such as composition of $HD^{16}O$ in the marsh water (discussed in section 3.4) and humidity, both exerting an influence on δD_F through the evaporation component (equations (2) and (3)).

Figure 8 compares the observed flux ratio with the predicted isotopic composition of evaporating vapor using the Craig-Gordon model (equation (3)). The tight correlation (a linear correlation coefficient 0.787 for data with good fetch and excluding observation at 1200 LT for SMEX–03) suggests that the Craig-Gordon model captured reasonably well the combined effect of equilibrium fractionation (first term of the numerator in (3)), atmospheric demand (second term), and kinetic effect (third term). The averaged values of the observed and modeled flux ratios are −103 and −111 per mil, respectively. The averaged value of δD_s from the same set of observations is −22 per mil. Substituting these numbers in (2) gives the fraction of transpiration of $F_T = 0.11$.

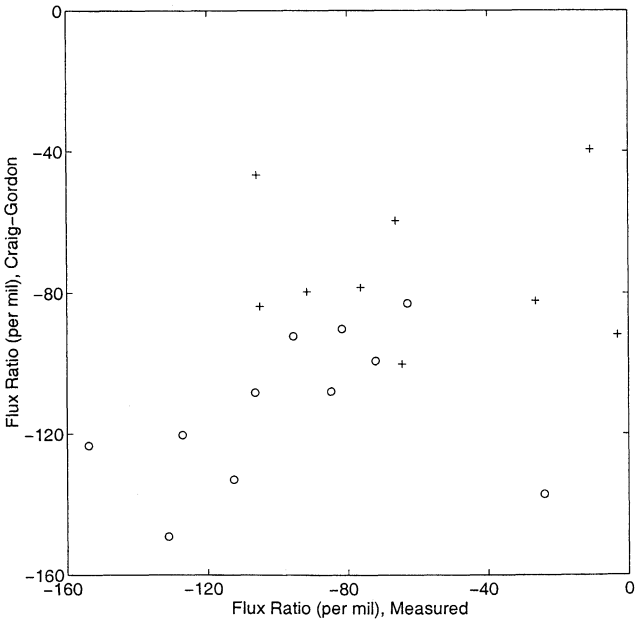

Figure 8. Comparison of observed flux ratio to flux ratio computed with the Craig-Gordon model (equation (3)) showing good fetch (circles) and poor fetch (pluses).

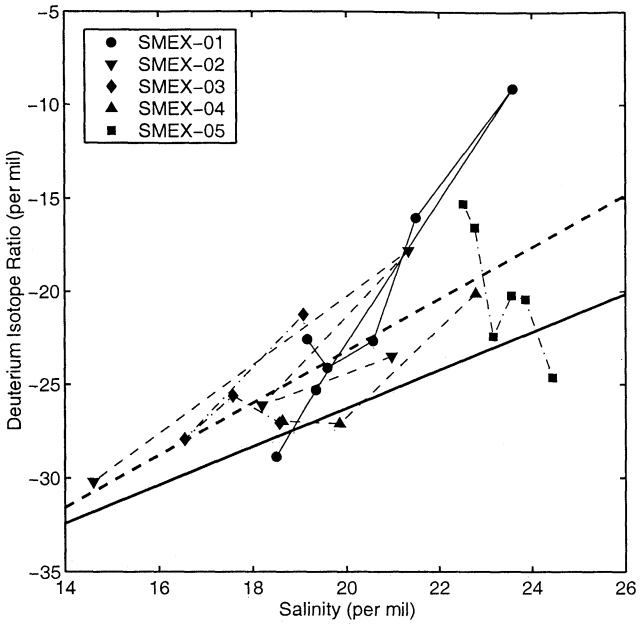

Figure 9. Plot of δD versus salinity S of water samples collected from the salt marsh for SMEX–01 (circles and line), SMEX–02 (triangles down and dashed line), SMEX–03 (diamonds and dot-dashed line), SMEX–04 (triangles up and dashed line), and SMEX–05 (squares and dot-dashed line). The bold dashed line is the least squares fit of the data, and the bold solid line is the mixing line formed by the ocean water and fresh lake water.

3.4. Salinity

Salinity, S, of the marsh surface water is given in Table 1. In Figure 9 the isotope ratio of the surface water, δD_s, is plotted against the corresponding S. The data points are rather scattered but show a general increase of δD_s with increasing S. A least squares fit of the data gives $\delta D_s = -51.1 + 1.39\,S$, with a goodness of fit $R^2 = 0.51$.

The relationship between δD_s and S is controlled by mixing of fresh on-land water and ocean water and by evaporative loss. Suppose that ocean and on-land water have isotope ratios of δD_0 and δD_1 and salinity values of S_0 and S_1, respectively. The mixing process can be represented by [*He,* 1998]

$$\delta D_s = \delta D_1 + \frac{\delta D_0 - \delta D_1}{S_0}\, S.$$

We collected a water sample from the tidal inflow of sea water from Long Island Sound and collected a freshwater sample upstream of the salt marsh on day 182 (July 1). Their isotope and salinity values are $\delta D_0 = -18.1$ per mil and $S_0 = 28.0 \times 10^{-3}$, and $\delta D_1 = -46.7$ per mil and $S_1 = 0$, respectively. Substituting these values into the above equation gives

$$\delta D_s = -46.7 + 1.02\,S. \tag{8}$$

This is plotted as the solid line in Figure 9, which appears to define a lower limit of the data region in the δD – S diagram. We argue below that the upward departure of the data points from this line is a result of evaporation.

To understand the temporal development of salinity and isotope ratio in the salt marsh, we assume that during flood tide the incoming ocean water mixes quickly with fresh water. If evaporation is negligible during this brief interval, the resulting mixture will fall on a mixing line shown in Figure 9. The times when the tide enters the marsh (and this mixture is established) are given in Table 2. After the mixing, three quantities will change with time because of evaporation: mass of water in the marsh, salinity, and isotope ratio of the marsh surface water. Now we can use the atmosphere-ocean exchange model developed by *He* [1998] to interpret the $\delta D_s - S$ relationship observed in the marsh water. For an isolated water body (and in the absence of precipitation), this is expressed as

$$\frac{d\delta D_s}{dS} = \frac{\delta D_s - \delta D_F}{S}, \tag{9}$$

where δD_F is the isotope flux ratio defined in (6), $d\delta D_s$ is the change in the isotope ratio of the marsh water over the period of observation, and dS is the change of marsh water salinity over the same period. Evaporation should make the ratio $d\delta D_s/dS$, which is the slope in the δD – S diagram, steeper than the envelope line in Figure 9 (see also (8)).

The observed slope can also be used to infer the isotope flux ratio. This is best illustrated with SMEX–01 data. Using its slope $d\delta D_s/dS$ of 3.65, mean δD_s of -21.2 per mil, and mean salinity of 20.3 per mil, (9) gives an estimate of δD_F of -95.5 per mil, which is in good agreement with our estimate using the gradient data (Table 1, yielding a mean of -87 per mil on the basis of four observations). Data from SMEX–02 to SMEX–04 give similar results, although the agreement is not as good as in SMEX–01.

The six samples from SMEX–05, however, show a general decreasing trend of δD_s with increasing salinity (Figure 9 and Table 1). The steady decrease of δD_s with time suggests a faster depletion of $HD^{16}O$ than of $H_2{}^{16}O$. This pattern is yet to be understood.

4. Conclusions

This paper reports the deuterium isotope ratios of atmospheric water vapor observed in the atmospheric surface layer above a coastal salt marsh. The study demonstrates the feasibility of the gradient diffusion or mixing

Table 2. Time Periods When Tidal Water Was Present at the Micrometeorological Mast (LT)

Experiment	First Tide	Second Tide
SMEX–01	0345 – 0730	1615 – 1830
SMEX–02	0655 – 0902	1845 – 2230
SMEX–03	0945 – 1245	2030 – 0022
SMEX–04	2330 – 0130	1130 – 1530
SMEX–05	0400 – 0830	1630 – 1945

line method in measuring the isotopic composition of the evapotranspiring water vapor at an ecosystem scale. Large scatters are, however, inevitable because the gradient of the isotopic composition in the surface layer is comparable to the analytical precision of the mass spectrometer. After imposing two objective data screening criteria (i.e., fetch requirement and transpiration constraint from (2)), we find that transpiration was a small component of the total evapotranspiration at the time of the experiment and that the Craig-Gordon model reproduced reasonably well the combined effect of equilibrium and kinetic fractionations and atmospheric demand on the evaporation process. Our study appears to be the first attempt at evaluating the Craig-Gordon model in field conditions.

We also show that temporal variations of salinity and the deuterium isotope ratio of the marsh water can be used to infer the isotope flux ratio. This may provide a useful alternative approach to determining δD_F without actually measuring δD of atmospheric water vapor.

Acknowledgments. The authors are grateful to John D. Kingston and Danny M. Rye who provided tremendous assistance in measuring the deuterium isotope ratio of water vapor and surface water samples and to Donald E. Aylor for thoughtful discussions on using critical orifice to restrain air flow into sampling canisters. Soo-Bum Chang assisted in salinity measurements. This research is supported in part by NSF research grant ATM-9121390 and National Institute for Global Environmental Change (NIGEC) grant 901214-HAR.

References

Bowling, D. R., D. D. Baldocchi, and R. K. Monson, Dynamics of isotopic exchange of carbon dioxide in a Tennessee deciduous forest, *Global Biogeochem. Cycles, 13,* 903-922, 1999.

Brunel, J. P., H. J. Simpson, A. L. Herezeg, R. Whitehead, and G. R. Walker, Stable isotope composition of water vapor as an indicator of transpiration fluxes from rice crops, *Water Resour. Res., 28,* 1407-1416, 1992.

Clark, I. D., and P. Fritz, *Environmental Isotopes in Hydrogeology,* 311 pp., CRC Press, Boca Raton, Fla., 1997.

Craig, H., and L. I. Gordon, Deuterium and oxygen 18 variations in the ocean and the marine atmosphere, in *Stable Isotopes in Oceanographic Studies and Paleotemperatures,* edited by E. Tongiorgi, pp. 9-130, Lab. di Geol. Nucl., Pisa, Italy, 1965.

Daneshyar, H., *One-Dimensional Compressible Flow,* 179 pp., Pergamon, New York, 1976.

Ehleringer, J. R., and T. E. Dawson, Water uptake by plants: Perspectives from stable isotope composition, *Plant Cell Environ., 15,* 1073-1082, 1992.

Flanagan, L. B., and J. R. Ehleringer, Effects of mild water stress and diurnal changes in temperature and humidity on the stable oxygen and hydrogen isotopic composition of leaf water in *Cornus stolonifera* L., *Plant Physiol., 97,* 298-305, 1991.

Friedman, I., A. C. Redfield, B. Schoen, and J. Harris, The variation of the deuterium content of natural waters in the hydrological cycle, *Rev. Geophys., 2,* 177-224, 1964.

He, H., Stable isotopes in the evaporating atmospheric water vapor, Ph.D. dissertation, 234 pp., Yale Univ., New Haven, Conn., 1998.

He, H., and R. B. Smith, Stable isotope composition of water vapor in the atmospheric boundary layer above the forests of New England, *J. Geophys. Res., 104,* 11,657-11,673, 1999a.

He, H., and R. B. Smith, An advective-diffusive isotopic evaporation-condensation model, *J. Geophys. Res., 104,* 18,619-18,630, 1999b.

Jouzel, J., Isotopes in cloud physics: Multiphase and multistage condensation processes, in *Handbook of Environmental Isotope Geochemistry,* vol. 2, edited by B. P. Fritz and J. C. Foutes, pp. 61-112, Elsevier Sci., New York, 1986.

Jouzel, J., and L. Merlivat, Deuterium and oxygen 18 in precipitation: Modeling of the isotopic effects during snow formation, *J. Geophys. Res., 89,* 11,749-11,757, 1984.

Jouzel, J., L. Merlivat, and C. Lorius, Deuterium excess in an East Antarctic ice core suggests higher relative humidity at the oceanic surface during the last glacial maximum, *Nature, 299,* 688-691, 1982.

Jouzel, J., C. Lorius, J. R. Petit, C. Genthon, N. I. Barkov, V. M. Kotlyakov, and V. M. Petrov, Vostok ice core: A continuous isotope temperature record over the last climate cycle (160,000 years), *Nature, 329,* 403-408, 1987.

Lee, X., G. Benoit, and X. Hu, Total gaseous mercury concentration and flux over a coastal salt marsh vegetation in Connecticut, USA, *Atmos. Environ., 34,* 4205-4213, 2000.

Merlivat, L., and J. Jouzel, Global climatic interpretation of the deuterium-oxygen 18 relationship for precipitation, *J. Geophys. Res., 84,* 5029-5033, 1979.

Roden, J., and J. R. Ehleringer, Observation of hydrogen and oxygen isotopes in leaf water confirms the Craig-Gordon model under wide-ranging environmental conditions, *Plant Physiol., 120,* 1165-1173, 1999.

Smith, R. B., Deuterium in North Atlantic storm tops, *J. Atmos. Sci., 49,* 2041-2057, 1992.

White, J. W. C., Stable hydrogen isotope ratios in plants: A review of current theory and some potential applications, in *Stable Isotopes in Ecological Research,* edited by P. W. Rundel, J. R. Ehleringer, and K. A. Nagy, pp. 142-162, Spinger-Verlag, New York, 1988.

White, J. W. C., and S. D. Gedzelman, The isotopic composition of atmospheric water vapor and the concurrent meteorological conditions, *J. Geophys. Res., 89,* 4937-4939, 1984.

Yakir, D., and L. S. L. Sternberg, The use of stable isotopes to study ecosystem gas exchange, *Oecologia, 123,* 297-311, 2000.

Yakir, D., and X. F. Wang, Fluxes of CO_2 and water fluxes between terrestrial vegetation and the atmosphere estimated from isotope measurements, *Nature, 380,* 515-517, 1996.

H. He, Raytheon Information Technology and Scientific Services, 4500 Forbes Boulevard, Lanham, MD 20706. (Hui_He@raytheon.com)

X. Lee, School of Forestry and Environmental Studies, Yale University, 370 Prospect Street, New Haven, CT 06511. (xuhui.lee@yale.edu)

R. B. Smith, Department of Geology and Geophysics, Yale University, P.O. Box 208109, New Haven, CT 06520-8109. (ronald.smith@yale.edu)

(Received July 28, 2000; revised January 15, 2001; accepted January 23, 2001.)